

# The $\theta_{Bn}$ problem: Determination of local magnetic parameters of interplanetary shocks from in situ IMF data

J. Américo González-Esparza<sup>1</sup> and Andre Balogh<sup>2</sup>

<sup>1</sup> Instituto de Geofísica, UNAM, México D.F., México

<sup>2</sup> Blackett Laboratory, Imperial College, London, United Kingdom

Received: June 2, 2000; accepted: October 3, 2000.

## RESUMEN

El ángulo  $\theta_{Bn}$  es el ángulo entre la normal de una onda de choque y el campo magnético en la región corriente arriba, y es un parámetro importante para el estudio de muchos fenómenos físicos relacionados con choques interplanetarios. Se muestra que no se puede inferir un valor confiable de  $\theta_{Bn}$  de una onda de choque interplanetaria sin estimar su incertidumbre asociada. Para cualquier choque interplanetario, siempre es posible inferir valores dispares de  $\theta_{Bn}$ . Se propone una sencilla técnica computacional para inferir un valor más confiable de  $\theta_{Bn}$  y determinar su incertidumbre. Esta técnica utiliza datos del campo magnético solamente y puede ser muy útil cuando no podemos aplicar las técnicas reiterativas que involucran necesariamente datos de plasma y campo magnético, y también puede aplicarse para estudiar otras discontinuidades MHD en el medio interplanetario. Para determinar  $\theta_{Bn}$  es necesario definir en la serie de datos una región corriente arriba y corriente abajo para aplicar las relaciones de conservación de Rankine-Hugoniot. Encontramos que el comportamiento fluctuante del campo magnético interplanetario, en particular su dirección, restringe la duración de estas regiones a tan sólo unos minutos antes y después del brinco del choque. Los choques cuasi-paralelos tienen un  $\theta_{Bn}$  con una mayor incertidumbre que los choques cuasi-perpendiculares. Cuando  $\theta_{Bn}$  tiene una incertidumbre grande se convierte en un parámetro dependiente del tiempo, el cual no tiene un valor bien definido, sino que está delimitado dentro de un rango de valores.

**PALABRAS CLAVE:** Física del medio interplanetario, ondas de choque interplanetarias, discontinuidades MHD.

## ABSTRACT

The angle  $\theta_{Bn}$  is the angle between the upstream magnetic field and the shock normal direction and is important for many phenomena in interplanetary physics. We show that for most shock observations,  $\theta_{Bn}$  cannot be determined without addressing its associated uncertainty. We propose a simple computational technique to infer a more reliable value for  $\theta_{Bn}$  and its associated uncertainty. This technique is based on magnetic field data only, and can be useful when we cannot apply the iterative techniques involving magnetic and plasma parameters. This method also can be applied to study other MHD discontinuities. To infer the shock local parameters, it is necessary to define upstream and downstream regions in the Rankine-Hugoniot relations. Fluctuations of the interplanetary magnetic field, particularly its direction, restrict the duration of these regions to just a few minutes before and after the shock. Quasi-parallel shocks have larger associated uncertainties than quasi-perpendicular shocks. When  $\theta_{Bn}$  has a large uncertainty, this angle becomes time dependent, i.e., does not have a well-defined value but varies within an angular range.

**KEY WORDS:** Interplanetary physics, interplanetary shocks, MHD discontinuities.

## INTRODUCTION

An interplanetary shock is a magnetohydrodynamic discontinuity (MHD) separating an upstream plasma ahead of the shock front (un-shocked medium) and a downstream plasma behind the shock (shocked medium). Ideally, having simultaneous plasma and magnetic field measurements with high temporal resolution on both sides of the discontinuity, we can apply the Rankine-Hugoniot (R-H) conservation equations. However, in practice when we want to use the R-H equations to infer the local characteristics of an interplanetary shock that passed by a spacecraft we have to assume that the successive in situ measurements of upstream and

downstream plasma and magnetic field parameters are time stationary.

In observational studies, the local shock parameters have to be deduced from the in situ upstream and downstream data series. Diverse methods to infer the shock local parameters and to verify the relationship between upstream and downstream values have been proposed [Colburn and Sonett, 1966; Abraham-Shrauner, 1972; Abraham-Shrauner and Yun, 1976; Chao *et al.*, 1984; Chao, 1985; Hsieh and Richter, 1986; Viñas and Scudder, 1986; Smith and Burton, 1988; Kessel *et al.*, 1994; Szabo, 1994]. These methods are based on different relationships deduced from the R-H equations and use

different subsets of plasma and magnetic field parameters. However, as the same authors report, these different methods have often led to disparate results of the shock parameters for the same set of observations. The arbitrary selection of the location and extension of the upstream and downstream regions has a strong influence on the shock parameters given by any method. When the solar wind parameters have fluctuations around the shock jump, small changes in selecting the upstream and downstream regions can produce significant differences in the solutions. In general, the data series of the solar wind plasma and magnetic field parameters have different time resolutions, while the available techniques require the same number of data points of magnetic and plasma parameters.

In this paper we discuss the determination of the shock local parameters from magnetic field data only. This is a relevant because, in general, the series of in situ magnetic field data have better time resolution and better accuracy than do the plasma moments (Song and Russell, 1999). Often only the magnetic field data are available for determining the shock local parameters. The analysis of the interplanetary shocks detected by the Ulysses spacecraft is a typical example of the problems that we found analyzing data elsewhere. The Ulysses solar wind plasma experiment has a 4 minutes sampling rate when the spacecraft is actively transmitting and 8 minutes during store periods (Bame *et al.*, 1992). This time resolution is too low to analyze the local parameters of most of the shocks observed by the spacecraft. On the other hand, the Ulysses magnetic field experiment has a time resolution of 1 or 2 seconds (Balogh *et al.*, 1992). There are 240 magnetic field vectors for each set of plasma moments. As a result, some characteristics of the shocks detected by Ulysses were determined mainly from the magnetic field data. This paper is concerned with the analysis of fast interplanetary shock waves (FISW), but the discussion can be extended to the study of other MHD discontinuities.

### THE MAGNETIC COPLANARITY THEOREM

The angle  $\theta_{Bn}$  is defined as the angle between the upstream magnetic field,  $\mathbf{B}_u$ , and the shock normal direction,  $\mathbf{n}_s$ , (Figure 1). Using this parameter we define a shock as parallel ( $\theta_{Bn} \approx 0^\circ$ ), quasi-parallel ( $0^\circ < \theta_{Bn} \leq 45^\circ$ ), quasi-perpendicular ( $45^\circ < \theta_{Bn} < 90^\circ$ ), and perpendicular ( $\theta_{Bn} \approx 90^\circ$ ). From a large-scale point of view, the R-H solutions depend on  $\theta_{Bn}$ , as this angle and the shock's strength determine how the shock transforms the medium [e.g., Kennel *et al.*, 1985]. From a microscopic point of view, the dissipation mechanism of an MHD collisionless shock changes dramatically with  $\theta_{Bn}$  (Kennel *et al.*, 1984; Goodrich, 1985). The origin of particle reflection and the acceleration of thermal particles associated with FISWs also depend on  $\theta_{Bn}$  (Lario *et al.*, 1998).

Figure 1 shows the discontinuity produced by an MHD fast shock wave in the magnetic field. The shock increases

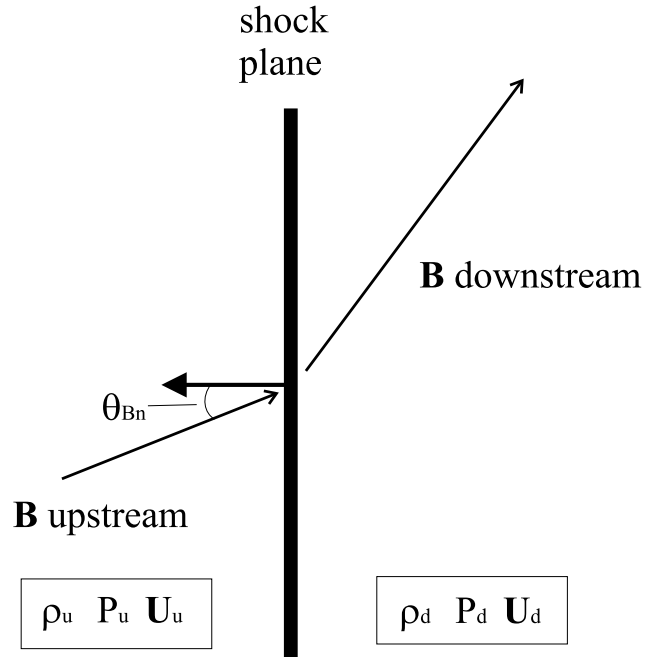


Fig. 1. Scheme of the shock's frame of reference showing a fast MHD shock wave propagating along the  $\mathbf{n}_s$  direction transforming irreversibly the upstream magnetic field  $\mathbf{B}_u$  to the downstream magnetic field  $\mathbf{B}_d$ . The angle  $\theta_{Bn}$  is the angle between the shock normal  $\mathbf{n}_s$  and the upstream magnetic field  $\mathbf{B}_u$ .

the component of the field parallel to the shock plane, while the normal field component is unaffected ( $B_{un} = B_{dn}$ ). In principle, continuity of the field's normal component ( $\nabla \cdot \mathbf{B} = 0$ ) has, among all the R-H equations, the least uncertainty for data series analysis since it is not affected by time variations. The magnetic coplanarity theorem states that for an oblique, compressive, fast MHD shock the upstream magnetic field,  $\mathbf{B}_u$ , the downstream magnetic field,  $\mathbf{B}_d$ , and the shock normal,  $\mathbf{n}_s$ , are all coplanar (Colburn and Sonett, 1966). The shock direction is obtained from the equation

$$\vec{n}_s = (\vec{B}_u - \vec{B}_d) \times (\vec{B}_u \times \vec{B}_d) .$$

This vector is then normalized to one. Note that this equation is not valid when the shock is exactly parallel ( $\theta_{Bn} = 0^\circ$ ), or when it is exactly perpendicular ( $\theta_{Bn} = 90^\circ$ ), since in both cases the upstream and downstream magnetic fields are parallel and thus ( $\vec{B}_u \times \vec{B}_d = 0$ ).

Figure 2 shows a geometrical interpretation of the coplanarity theorem. The three vectors  $\mathbf{B}_u$ ,  $\mathbf{B}_d$ , and  $(\mathbf{B}_d - \mathbf{B}_u)$ , form a triangle contained in the coplanarity plane. The angle  $\alpha$  is the angle between the upstream and downstream magnetic field, i.e., the angular deflection caused by the shock to the field. As  $(\mathbf{B}_d - \mathbf{B}_u)$  is orthogonal to  $\mathbf{n}_s$ ,  $\theta_{Bn}$  can be drawn inside the triangle. Applying sine and cosine laws in Figure 2 we obtain:

$$\theta_{Bn} = \arccos\left(\frac{\sin \alpha}{\sqrt{1 + r_B^2 - 2r_B^{-1} \cos \alpha}}\right), \quad (1)$$

where  $r_B$  is the magnetic field magnitude compression ratio:  $r_B = B_d / B_u$ . This equation is similar to the one by Chao *et al.*, 1984, and shows that when we want to infer the  $\theta_{Bn}$  angle for a FISW, the angular deflection  $\alpha$  and the jump in the field's magnitude  $r_B$  caused by the shock must be well-defined in the IMF data. Note that we obtain  $\theta_{Bn}$  without inferring the shock normal. In parallel and perpendicular shocks the deflection angle  $\alpha$  is equal to zero; but in parallel shocks  $r_B=1$  and in perpendicular shocks  $r_B>1$ . Thus we can infer any  $\theta_{Bn}$  using Equation 1. When the jump in field's magnitude is small (e.g.,  $r_B < 1.3$ ),  $\theta_{Bn}$  becomes very sensitive to small variations in  $\alpha$ ; such shocks are more difficult to analyze. For a given  $r_B$ , smaller values of  $\alpha$  are related to quasi-perpendicular shocks and large  $\alpha$  values to quasi-parallel shocks. In the next section we discuss some problems for inferring shock local magnetic parameters from in situ data.

### THE $\theta_{Bn}$ PROBLEM

Figure 3 shows a FISW detected by the magnetic field experiment on board Ulysses on day 91:199. The 20-minute plots show the three spherical coordinates of the IMF: latitudinal ( $\Theta$ ) and longitudinal ( $\Phi$ ) angles, and field magnitude ( $|B|$ ). One IMF vector was obtained every 2 seconds. The

### Geometrical Interpretation of the Magnetic Coplanarity

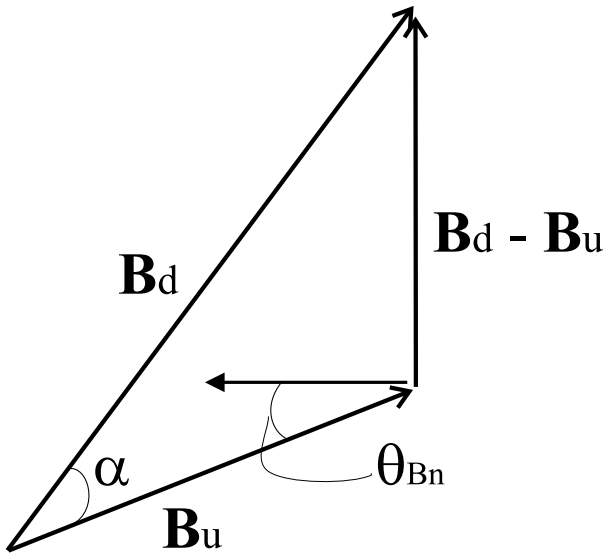


Fig. 2. Geometrical interpretation of the coplanarity theorem. The upstream magnetic field  $\mathbf{B}_u$ , the downstream magnetic field  $\mathbf{B}_d$ , and the shock normal  $\mathbf{n}_s$  lie in the same plane. The angle  $\alpha$  is the deflection in the magnetic field caused by the shock discontinuity.

jump in  $|B|$  is well-defined and the IMF magnitude is very quiet on both sides of the shock. However, from the plots of the spherical angles, it is practically impossible to tell where the shock jump occurred.

Consider now the shock local magnetic parameters. In general, when we apply the coplanarity technique to infer these parameters we average two arbitrary intervals just before and after the shock to determine the  $r_B$  and  $\alpha$  values attributed to the shock. From these two parameters, we use Equation 1 to obtain the value of  $\theta_{Bn}$ . This method produces contradictory results as may be shown in the following. Suppose that we take an interval of 10 minutes just before and another 10-minute interval just after the shock. Each 10-minute interval is subdivided into 10 subintervals of 1 minute. By averaging these subintervals we obtain 10 IMF upstream vectors and an equal number of IMF downstream vectors. In principle, there is no obvious reason to prefer one subinterval to any other and any IMF vector represents the whole interval as well as any other. We take the first IMF upstream vector and combine it with all 10 IMF downstream vectors; thus from Equation 1 we find values of 10  $\theta_{Bn}$ . We repeat the same procedure for the second IMF upstream vector, inferring another 10 values of  $\theta_{Bn}$  and so on. At the end of these calculations we will have all possible values of  $\theta_{Bn}$ , equal to 10 times 10 (100) values of  $\theta_{Bn}$ .

Figure 4 shows the scatter plot of the 100 values of  $\theta_{Bn}$  that were obtained in this fashion. This collection of values of  $\theta_{Bn}$  shows that it is possible to characterize this shock either as a quasi-parallel shock with a  $\theta_{Bn} \approx 30^\circ$  or a quasi-perpendicular shock with a  $\theta_{Bn} \approx 86^\circ$ . The difference is due to the arbitrary selection of the upstream and downstream location that defines the values of  $\alpha$  and  $r_B$  attributed to the shock. We call this uncertainty ‘the  $\theta_{Bn}$  problem’. The arbitrary number of subintervals subdividing the upstream and downstream regions is unimportant. The point is that in most interplanetary shocks it is possible to find arbitrary combinations between upstream and downstream IMF vectors leading to a wide range of  $\theta_{Bn}$  values.

The IMF deflection produced by the shock discontinuity  $\alpha$  is superposed on other directional variations propagating through the field. In many cases these variations are larger than  $\alpha$  and it is very difficult to locate the shock discontinuity in the IMF angular plots. In terms of magnetic observations, the shock shown in Figure 3 is a quasi-laminar shock with a sharp transition and relatively quiet upstream and downstream regions. Thus even with simple shocks, the ‘ $\theta_{Bn}$  problem’ arises. In general, interplanetary shocks can have very noisy magnetic transitions in terms of magnitude and field direction, and their profiles can look very different from each other.

In order to illustrate further the ‘ $\theta_{Bn}$  problem’, Figure 5 shows another FISW detected by Ulysses magnetometer on

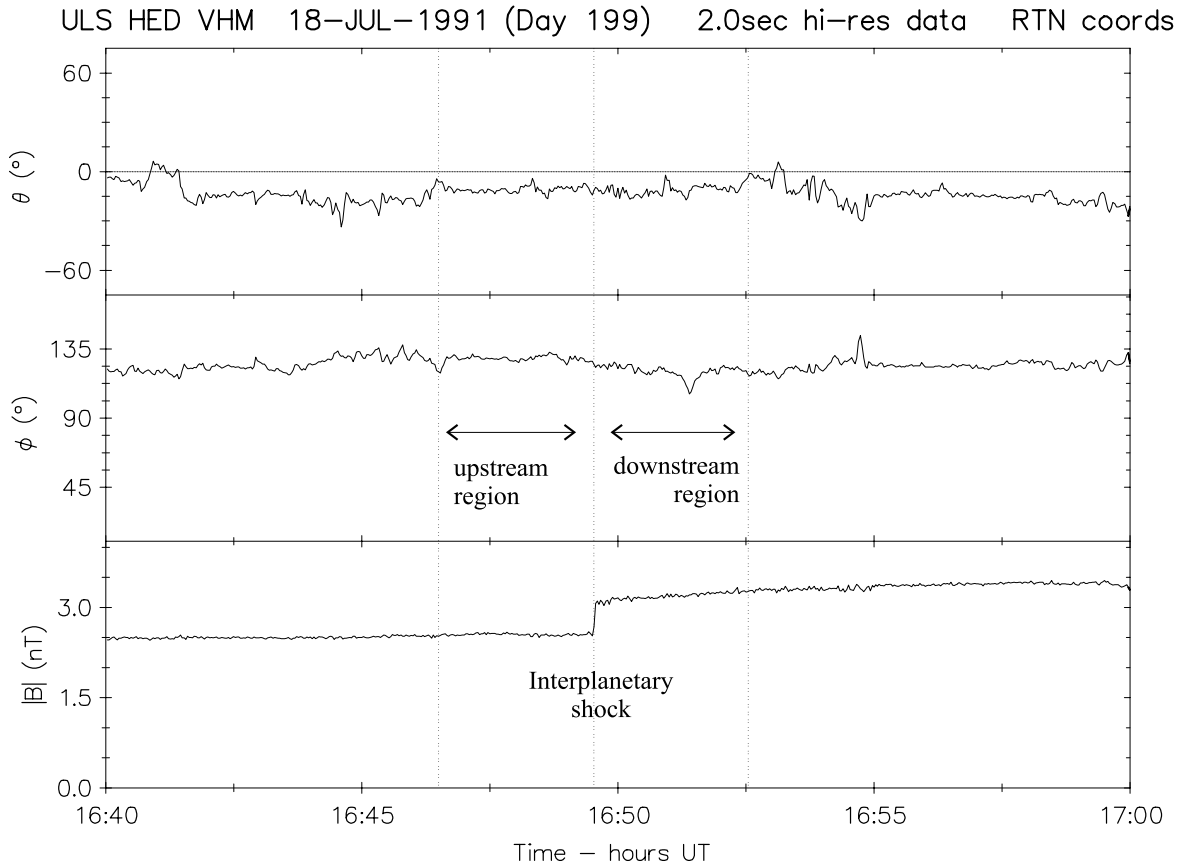


Fig. 3. Interplanetary shock wave detected by Ulysses magnetometer on day 91:199. The event is shown in RTN spherical coordinates. *a)* latitudinal angle ( $\Theta$ ), *b)* longitudinal angle ( $\Phi$ ), *c)* magnetic field magnitude ( $|B|$ ).

day 97:115, in spherical coordinates. As like in the previous shock, the jump in magnitude is well-defined, but the behavior of the two IMF spherical angles is ambiguous. We repeat the same process as before taking an upstream and downstream region of 10 minutes and subdividing these regions in 10 subintervals of 1 minute. As described before we averaged these subintervals and combined all the 10 upstream and 10 downstream IMF vectors obtaining 100 values of  $\theta_{Bn}$ . Figure 6 shows the scatter plot of the 100 values of  $\theta_{Bn}$  versus their deflection angle  $\alpha$ . In this case it is possible to characterize the shock with a  $\theta_{Bn}$  from  $56^\circ$  to  $89^\circ$ . There is the same problem: variations in the parameters describing the magnetic changes attributed to the shock produce the dispersion in the values of  $\theta_{Bn}$ . In Balogh *et al.*, 1995, (here after paper 1) we used a similar ensemble technique to obtain the  $\theta_{Bn}$  values of 160 FISWs detected by Ulysses magnetometer from 1990 to 1993. We found, with different severity in each case, the same problem in most of the shocks.

#### ESTIMATION OF THE ASSOCIATED UNCERTAINTY OF $\theta_{Bn}$

What can be done to improve the determination of  $\theta_{Bn}$  and infer a more reliable value? In this section we propose a

computational technique based on four steps: (a) selection of the initial upstream and downstream regions and subdividing these regions to produce an arbitrary number of averaged IMF vectors; (b) combination of the upstream and downstream IMF vectors to build 'ensemble' distributions of possible values of the local magnetic field parameters:  $\alpha$ ,  $r_B$ , and  $\theta_{Bn}$ ; (c) statistical analysis of these distributions; and (d) reiteration of the whole process varying the extension of the upstream and downstream regions to find the better solution and test the stability of the results.

#### a) Upstream and downstream regions

The initial upstream and downstream regions in the IMF data series are defined in such a way as to comprise the maximum extension before / after the shock transition (avoiding foot, ramp, and overshoot) where the changes in the IMF magnitude ( $r_B$ ) and direction ( $\alpha$ ) are mainly associated with the shock and not with other phenomena in the solar wind. For consistency, the two regions should have the similar extensions. The shock shown in Figure 3 shows how the initial upstream and downstream intervals are selected. The shock occurred at  $\approx$ UT 16:49 and caused a small but well defined jump in  $|B|$ . The IMF directional behavior is less clear and

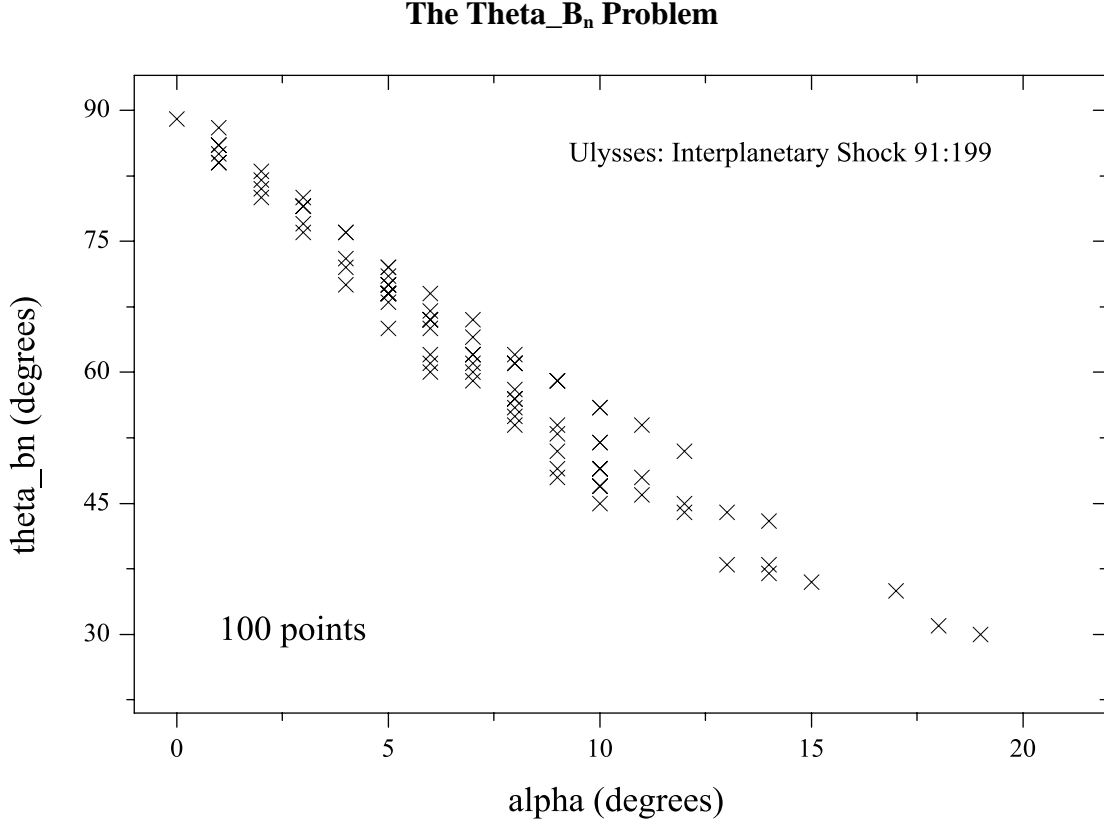


Fig. 4. Scatter plot of 100  $\theta_{Bn}$  's obtained by the different combinations of upstream / downstream magnetic field vectors for the shock shown in Figure 3. See the text for details. Arbitrary selections of upstream and downstream regions produce different results for  $\theta_{Bn}$ .

there is no a well defined angular deflection associated with the jump. Eye-scanning the plot we note that about 3 minutes before the shock jump ( $\approx$ UT 16:46) there is a deflection in both angles which cannot be attributed to the shock discontinuity and the directional behavior is different before that point. Since this angular deflection is significantly larger than the rotation ( $\alpha$ ) associated with the shock, this deflection restricts the duration of the upstream region. For consistency, the initial downstream region is defined with the same extension. For this shock this angular deflection that was not directly related to the shock jump, determines the extension of the initial upstream and downstream regions. In other shocks, changes in the IMF magnitude ( $|B|$ ) may constrain the extension of the regions. González-Esparza, 1995, found that in general, on the basis of the criteria described before, the upstream and downstream IMF regions had a temporal length of less than five minutes. This is important when we combine data series of solar wind plasma and magnetic field parameters with different temporal resolutions.

### b) Ensemble distributions

After selecting the initial upstream and downstream regions, we divide the two regions into an arbitrary number of subintervals. From our experience, 10 subintervals on each

region is a good number to obtain the statistical analysis. We average these subintervals to 'filter' the high frequency noise and get a set of (10) upstream and (10) downstream IMF vectors. As before, we combine each upstream and downstream vector to obtain a value of:  $\alpha$ ,  $r_B$ , and  $\theta_{Bn}$ . After combining all the vectors we get an ensemble data set of the three shock magnetic parameters. Similar to Viñas and Scudder, 1986, the statistical analysis of these data sets indicates whether the upstream and downstream regions, and the changes caused by the shock, were well-defined in the IMF data.

### c) Statistical Analysis

From our analysis of 145 FISWs detected by Ulysses we found that when the upstream and downstream regions were well-defined in the IMF data series, the data sets of  $\alpha$ ,  $r_B$ , and  $\theta_{Bn}$  tend to be approximately normally distributed [González-Esparza, 1995]. Confidence that the normal approximation is adequate comes from a variety of sources, in particular we use the skewness factor,  $g_1$ :

$$g_1 = \frac{\sum_{i=1}^n (x_i - \bar{x})^3}{n\sigma^3}, \quad (2)$$

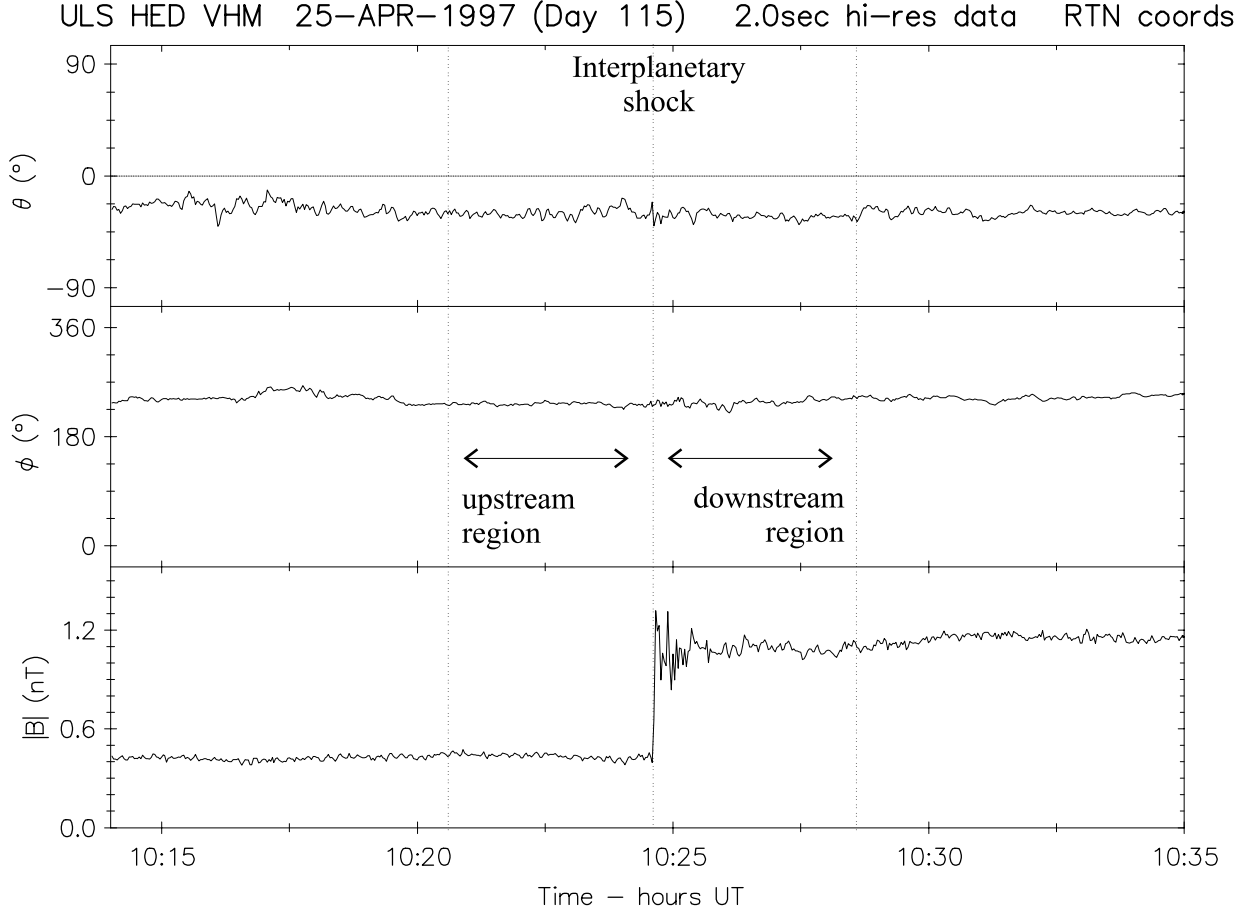


Fig. 5. Interplanetary shock wave detected by Ulysses magnetometer on day 97:115.

and the kurtosis factor,  $g_2$ :

$$g_2 = \frac{\sum_{i=1}^n (x_i - \bar{x})^4}{n\sigma^4} - 3, \quad (3)$$

(where  $n$  is the total number of data points (in this case  $n=100$ ), and  $\bar{x}$  and  $\sigma$  are the mean value and standard deviation of the distribution, respectively). The factor  $g_1$  indicates if the data are unsymmetrically distributed around the mean, and  $g_2$  indicates if the data are abnormally compressed or are more spread out than for a true normal distribution. For a perfect normal distribution  $g_1$  and  $g_2$  are equal to zero. In our technique we chose the set of ensemble distributions ( $\theta_{Bn}$ ,  $\alpha$ , and  $r_B$ ) with the best values for these two factors.

#### d) Stability of the solutions

In order to be confident that the technique is reliable, the results from the distributions should be stable and the data points randomly distributed around the mean. As noted above, we expect the three data sets ( $\theta_{Bn}$ ,  $\alpha$ , and  $r_B$ ) to be approximately normally distributed. The values of  $g_1$  and  $g_2$

give us two quantitative parameters to determine how good the normal approximation is for each data set. The selection of the upstream and downstream regions can be very difficult and debatable in many cases. We reiterate the whole process a few times (e.g., 5) gradually reducing the extension of the initial upstream and downstream regions to obtain other values of  $g_1$  and  $g_2$  for each parameter. We define the ‘best solution’ with the upstream and downstream regions that give us the best possible values of  $g_1$  and  $g_2$  for each parameter, in particular for the  $\theta_{Bn}$  distribution. This reiteration also helps us to verify the stability of the different solutions that should agree to a reasonable degree. From the ‘best solution’, we define the ‘best value’ for  $\theta_{Bn}$  as the mean of its distribution ( $\bar{\theta}_{Bn}$ ) and its associated uncertainty as the standard deviation of its distribution ( $\Delta\theta_{Bn}=\sigma_\theta$ ).

The method assumes that there are well-defined changes in the IMF magnitude and direction related to the shock and these changes can be inferred from the upstream and downstream IMF data. Note however that there are some shocks where we cannot find well-defined normal distributions and the associated uncertainties are very large. For those shocks  $\theta_{Bn}$  is time dependent.

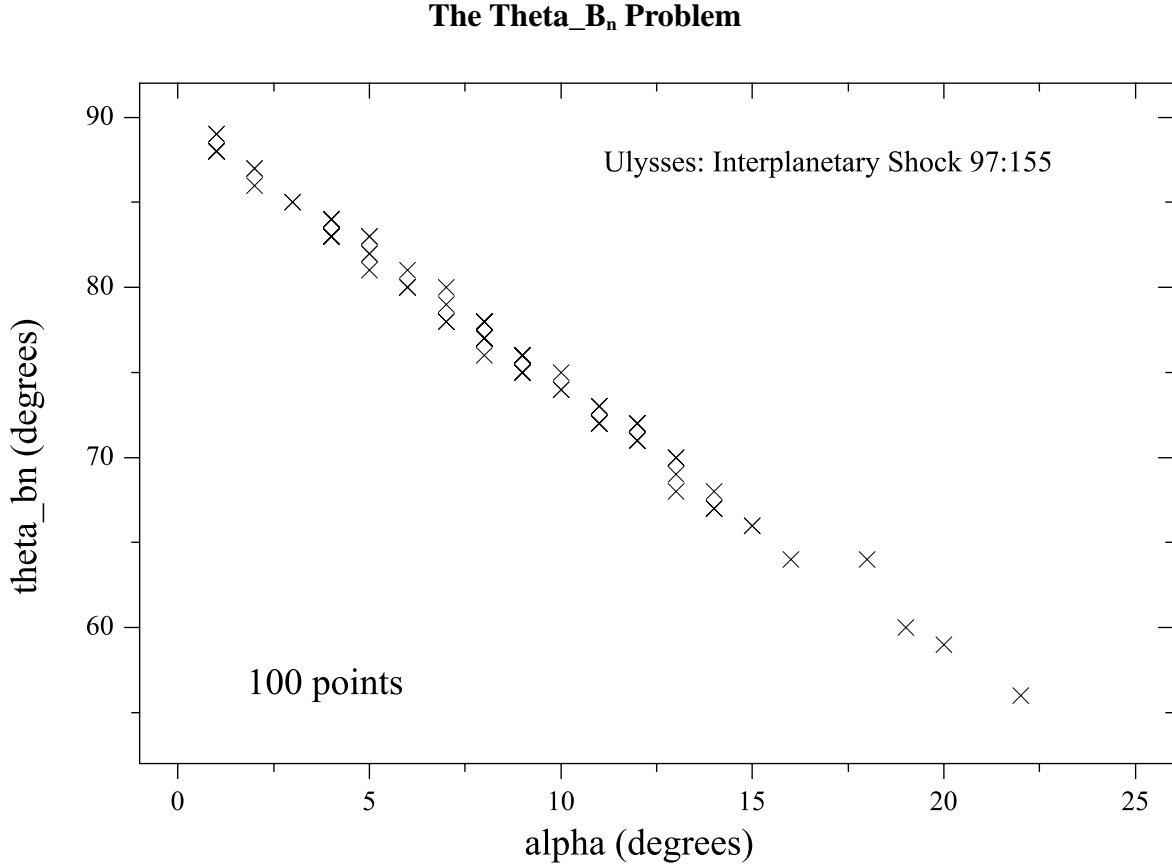


Fig. 6. Scatter plots of 100  $\theta_{Bn}$ 's obtained by the different combinations of upstream / downstream magnetic field vectors for the shock shown in Figure 5. See the text for details.

## RESULTS

Figure 7 shows the histograms of  $r_B$ ,  $\alpha$ , and  $\theta_{Bn}$  of the best solution of the shock wave detected by Ulysses on day 91:199 (Figure 3). From the reiterative process we found that the extension of the 'best' upstream and downstream regions were about two minutes. Superposed onto each histogram there is a Gaussian curve defined by the mean value and the standard deviation of the corresponding data series. The  $r_B$  histogram in Figure 7 shows that the jump in  $|B|$  was relatively well-defined, but there is an excess of higher values in the distribution ( $g_1 > 0$ ), and the kurtosis factor ( $g_2 < 0$ ) tell us that this distribution is sharper than the normal distribution. On the other hand, the  $\alpha$  histogram shows that the deflection caused by the shock had a significant uncertainty. The best value for  $\theta_{Bn}$  was  $51^\circ$  with an uncertainty of  $11^\circ$ . We should keep in mind that  $\alpha$  and  $r_B$  are determined directly from the IMF data, whereas  $\theta_{Bn}$  is calculated from these two parameters using Equation 1. The uncertainties of the first two parameters affect the calculation of  $\theta_{Bn}$ . As stated above, shocks with a small  $r_B$  tend to be more difficult to analyze.

Figure 8 shows the histograms of  $r_B$ ,  $\alpha$ , and  $\theta_{Bn}$  of the

best solution for the shock wave detected by Ulysses on day 97:155 (Figure 5). In this case, the extensions of the 'best' upstream and downstream regions were also about two minutes. The  $r_B$  histogram in Figure 8 shows that the jump in  $|B|$  was larger and better defined than for the previous shock. The values of  $g_1$  and  $g_2$  were very small denoting that in this case the normal approximation was very good. The  $\alpha$  histogram shows that the deflection caused by the shock was small, but it was also well defined. The best value for  $\theta_{Bn}$  was  $81^\circ$  with an associated uncertainty of  $5^\circ$ .

In paper 1 we used a similar ensemble to technique to report the  $\theta_{Bn}$  value and their associated uncertainty of 160 FISWs detected by Ulysses. However, the results in paper 1 were obtain in terms of qualitative judgment where the ensemble distributions had to compare 'favorably' to Gaussian fits. In this case we propose a quantitative procedure, given by the  $g_1$  and  $g_2$  factors, that defines which is the best distribution. When we repeated the analysis of the 160 shocks reported in paper 1 using this new approach, we found a very good agreement in all the cases. For example, the shock detected by Ulysses on day 91:199 was reported in paper 1 with a  $\theta_{Bn} = 53^\circ \pm 10^\circ$ ; and in this paper, using the  $g_1$  and  $g_2$ ,

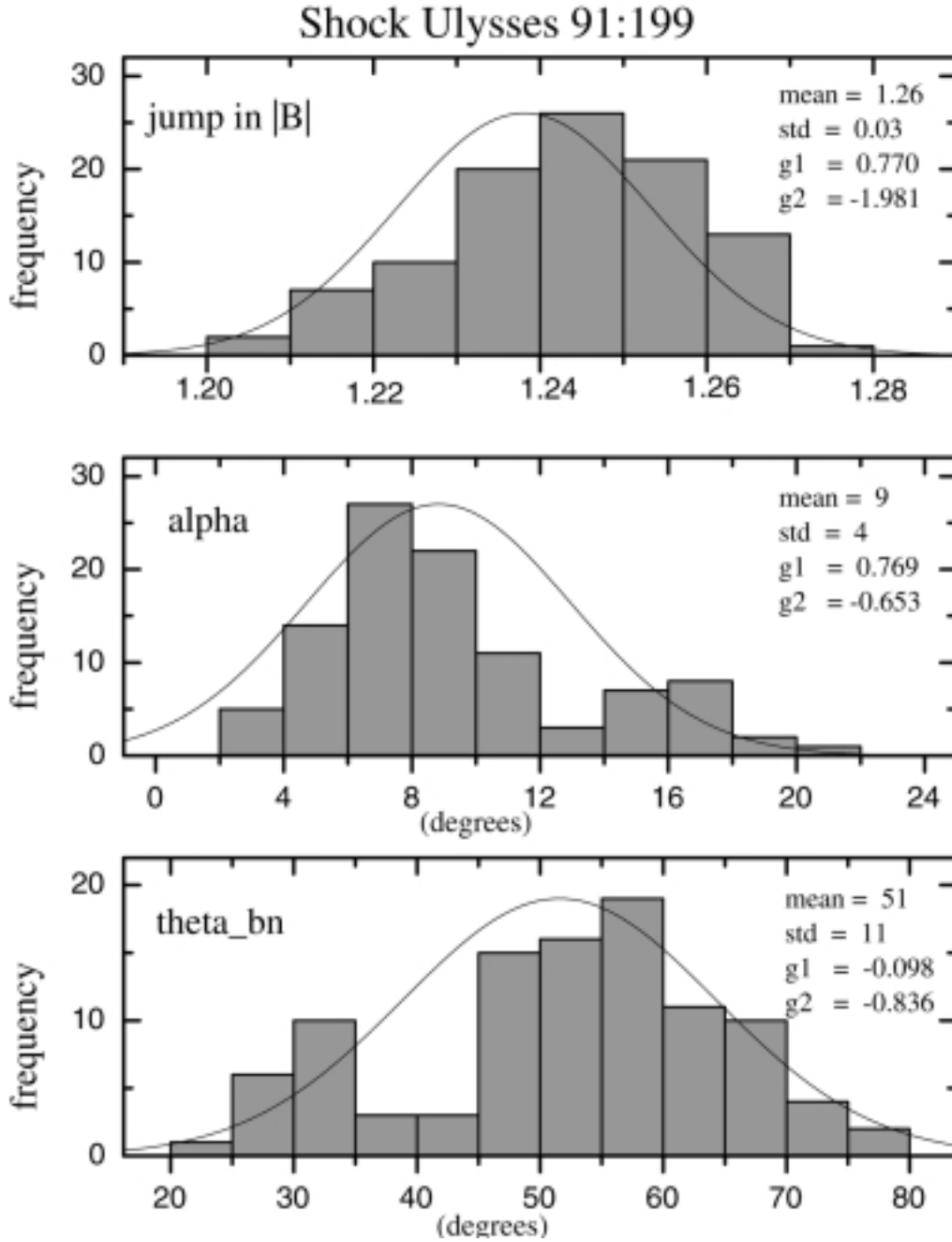


Fig. 7. Histogram distributions for the three local magnetic parameters:  $r_B$ ,  $\alpha$ , and  $\theta_{Bn}$ , associated with the best solution of the shock on day 91:199 (Figure 3). See the text for details. The mean value of the  $\theta_{Bn}$  distribution defines its best possible value and its standard deviation defines its uncertainty.

factors with a  $\theta_{Bn} = 51^\circ \pm 11^\circ$ . This shows again the importance of the error analysis.

## 6. DISCUSSION AND CONCLUSIONS

The angle  $\theta_{Bn}$  is important for many phenomena in interplanetary physics. In this paper we presented two examples showing that the angle  $\theta_{Bn}$  cannot be determined without ad-

ressing the associated uncertainties. The study of a large set of interplanetary shocks detected by the Ulysses magnetometer shows that this is true in general. The fluctuating behavior of the interplanetary magnetic field and the perturbations attributed to the internal processes of collisionless shocks produce an uncertainty in the estimation of the shock parameters. The error analysis of  $\theta_{Bn}$  is not only necessary in terms of rigorous reporting, but the uncertainty associated



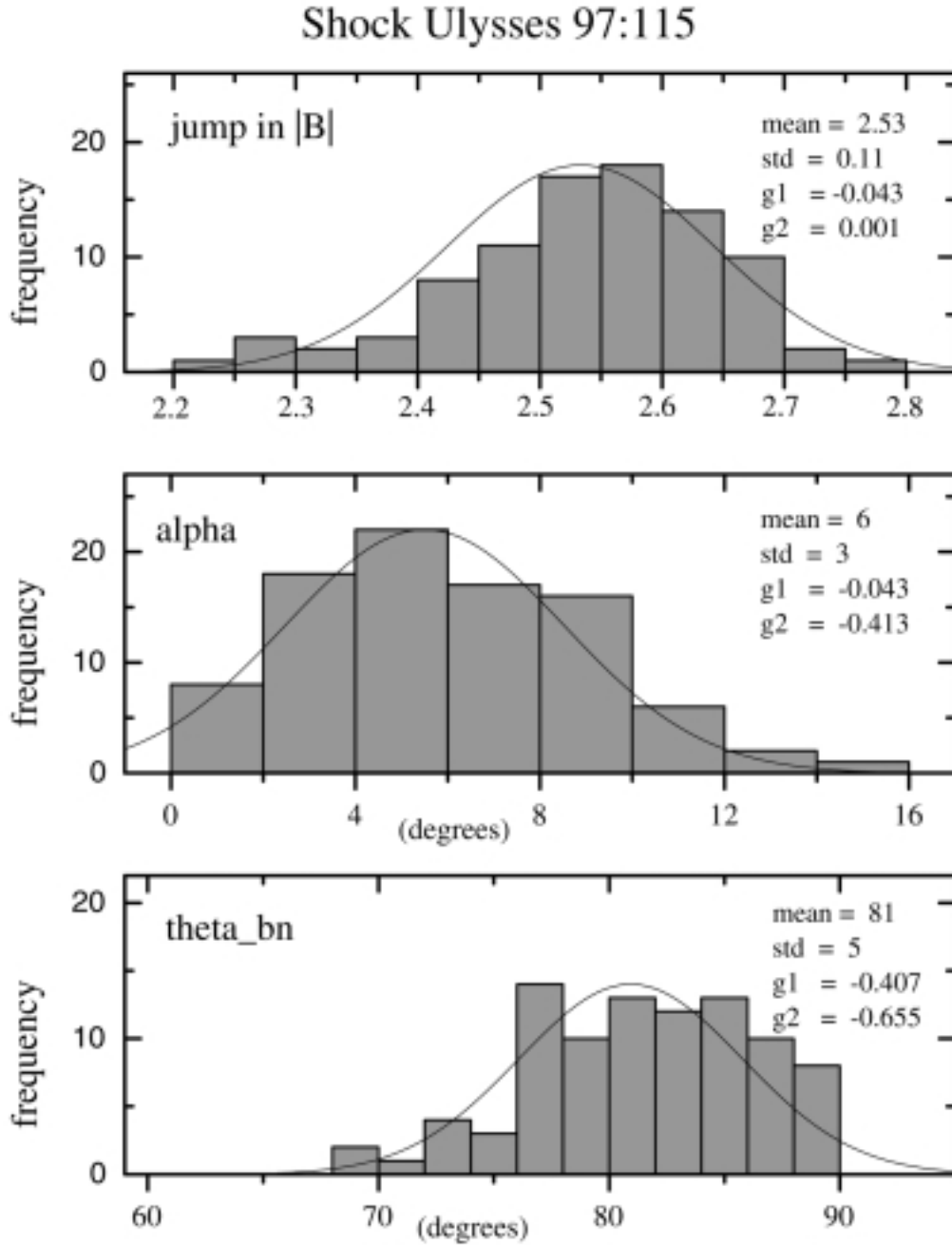


Fig. 8. Histogram distributions for the three local magnetic parameters:  $r_B$ ,  $\alpha$ , and  $\theta_{Bn}$ , associated with the best solution of the shock on day 97:155 (Figure 5).

with  $\theta_{Bn}$  is part of the physical processes of the collisionless shock itself.

We showed the ambiguous behavior of the IMF direction through the shock discontinuity, it is very difficult to locate the shock in the angular plots. The deflection of the magnetic field produced by the shock is superposed with other directional variations propagating through the field, and in most cases these variations are larger than  $\alpha$ .

We propose a simple technique to improve the estimation of  $\theta_{Bn}$  and its associated uncertainty using IMF data. The confidence of this technique is based on the study of 160 FISWs detected by Ulysses magnetometer from 1990 to 1993 (paper 1) and 78 FISWs detected from 1996 to 1998.

In general, shocks with a large  $\theta_{Bn}$  ( $\geq 80^\circ$ ) have a well-defined shock discontinuity and the angle  $\theta_{Bn}$  can be inferred with a small associated uncertainty ( $\leq 5^\circ$ ). However, when

the angle is less than  $60^\circ$  the associated uncertainty can be large ( $\geq 10^\circ$ ). This uncertainty is produced by the waves and reflected particles related to the shock perturbing the upstream and downstream regions. These perturbations cause continual variations in the ambient IMF direction and  $\theta_{Bn}$  becomes time dependent. In these cases the angle  $\theta_{Bn}$  cannot be thought of as a single value but as a varying parameter within an angular range. The assumption of a stationary system supporting the applicability of the Rankine-Hugoniot relations can be debatable.

Finally, it is important to emphasize the local nature of the shock parameters determined from single spacecraft observations. The fluctuating behavior of the IMF, in particular its direction, restricts the duration of the upstream and downstream regions relevant to the local shock parameters to just a few minutes before and after the shock. Under ideal conditions (solar wind plasma and magnetic field data series with no gaps and the same temporal resolution) the reiterative-techniques involving magnetic and plasma parameters (Viñas and Scudder, 1986; Kessel *et al.*, 1994; Szabo, 1994) are the best option to infer the shock local characteristics. However, for many shock observations the plasma data has a low time resolution or, in some cases, it can be missing altogether, and then the magnetic field data becomes the only option to infer the shock local magnetic parameters.

#### ACKNOWLEDGMENTS

We are grateful to Pete Riley for many useful discussions. Comments and suggestions by the referees are acknowledged.

#### BIBLIOGRAPHY

- ABRAHAM-SHRAUNER, B., 1972. Determination of Magnetohydrodynamic Shock Normal. *J. Geophys. Res.*, *77*, 736.
- ABRAHAM-SHRAUNER, B. and S. H. YUN, 1976. Interplanetary shocks seen by Ames Plasma probe on Pioneer 6 and 7, *J. Geophys. Res.*, *81*, 2097.
- BALOGH, A., T. J. BEEK, R. J. FORSYTH, P. C. HEDGECOCK, R. J. MARQUEDANT, E. J. SMITH, D. J. SOUTHWOOD and B. T. TSURUTANI, 1992. The magnetic field investigation on the Ulysses mission: instrumentation and preliminary scientific results. *Astron. Astrophys. Suppl. Series*, *92*, 221-236.
- BALOGH, A., J. A. GONZALEZ-ESPARZA, R. J. FORSYTH, M. E. BURTON, B. E. GOLDSTEIN, E. J. SMITH and S. T. BAME, 1995. Interplanetary Shock Waves : Ulysses Observations In and Out of the Ecliptic Plane. *Space Sci. Rev.*, *72*, 171-180. (Paper 1)
- BAME, S. J., D. J. MCCOMAS, B. L. BARRCLOUGH, J. L. PHILLIPS, K. J. SOFALY, J. C. CHAVEZ, B. E. GOLDSTEIN and R. K. SAKUR. The Ulysses mission solar wind plasma experiment. *Astron. Astrophys. Suppl. Series*, *92*, 237-265.
- COLBURN, D. and C. P. SONETT, 1966. Discontinuities in the Solar Wind. *Space Sci. Rev.*, *5*, 439.
- CHAO, J. -K. and K. C. HSIEH, 1984. On Determining Magnetohydrodynamics Shock Parameters  $\theta_{Bn}$  and  $M_A$ . *Planetary Space Sci.*, *32*, 641.
- CHAO, J. -K., 1985. Intermediate shocks: observations. *Adv. Space Sci.*, *15* (8/9), 521-530.
- DRYER, M., 1994. Interplanetary studies: propagation of disturbances between the sun and the magnetosphere. *Space Sci. Rev.*, *67*, 363.
- GOODRICH, C. C., 1985. Numerical simulations of quasi-perpendicular collisionless shocks. *In: Collisionless Shocks in the Heliosphere: Reviews of Current Research*, Geophys. Monogr. Ser., *35*, edited by R. G. Stone and B. T. Tsurutani, pp. 153-168, AGU, Washington, D. C.
- GONZALEZ-ESPARZA, J. A., 1995. Study of Heliospheric Shock Waves Observed by Ulysses Magnetometer In and Out of the Ecliptic Plane, Ph.D. thesis, 226 pp., Imperial College., London, January.
- HSIEH, K. C. and A. K. RICHTER, 1986. The Importance of Being Earnest About Shock Fitting. *J. Geophys. Res.*, *91*, 4157.
- KENNEL, C. F., F. L. SCARF, F. V. CORINITI, C. T. RUSSELL, K.P. WENZEL, T.R. SANDERSON, P. VAN NES, W. C. FELDMAN, G. K. PARKS, E. J. SMITH, B. T. TSURUTANI, F. S. MOZER, M. TEMERIN, R. R. ANDERSON, J. D. SCUDDER and M. SCHOLER, 1984. Plasma and energetic particle structure upstream of a quasi-parallel interplanetary shock. *J. Geophys. Res.*, *89*, 5419.
- KENNEL, C.F., J.P. EDMISON and T. HADA, 1985. A quarter century of collisionless shock research. *In: Collisionless Shocks in the Heliosphere: A Tutorial Review*. Geophys. Monogr. Ser., *34*, edited by R. G. Stone and B. T. Tsurutani, pp. 1-36, AGU, Washington, D. C.

KESSEL, R., A. J. COATES, U. MOTSCHMANN and F. M. NEUBAUER, 1994. Shock normal determination for multi-ion shocks. *J. Geophys. Res.*, *99*, 19359-19374.

LARIO, D., B. SANAHUJA and A. M. HERAS, 1998. Energetic particle events: efficiency of interplanetary shocks as  $50 \text{ keV} < E < 100 \text{ MeV}$  proton accelerators. *Astrophys. J.*, *509*, 415-434.

SMITH, E. J. and M. E. BURTON, 1988. Shock Analysis: Three Useful New Relations. *J. Geophys. Res.*, *93*, 2730-2734.

SONG, P. and C. TRUSSELL, 1999. Time series data analyses in space physics. *Space Sci. Rev.*, *87*, 387-463.

SZABO, A., 1994. An improved solution to the 'Rankine-Hugoniot' problem. *J. Geophys. Res.*, *99*, 14,737-14746.

VIÑAS, A. F. and J. D. SCUDDER, 1986. Fast and Optimal Solution to the "Rankine-Hugoniot Problem". *J. Geophys. Res.*, *91*, 39.

---

J. Américo González-Esparza<sup>1</sup> and Andre Balogh<sup>2</sup>

<sup>1</sup> Instituto de Geofísica, UNAM, 04510 México, D.F., México  
Email: americo@fis-esp.igeofcu.unam.mx

<sup>2</sup> Blackett Laboratory, Imperial College, London,  
United Kingdom